



OPEN ACCESS

EDITED BY
Hua Chen,
Guangxi Normal University, China

REVIEWED BY
Zhiqiang Mao,
Hubei University, China
Yang Qinglai,
University of South China, China

*CORRESPONDENCE
Hongwen Liu,
liuhongwen@hnu.edu.cn
Kang Chen,
chenkang@hunnu.edu.cn
Haixia Li,
472176061@qq.com

SPECIALTY SECTION
This article was submitted to Biosensors
and Biomolecular Electronics,
a section of the journal
Frontiers in Bioengineering and
Biotechnology

RECEIVED 13 October 2022
ACCEPTED 01 November 2022
PUBLISHED 23 November 2022

CITATION
Chen X, Yuwen Z, Zhao Y, Li H, Chen K
and Liu H (2022), *In situ* detection of
alkaline phosphatase in a cisplatin-
induced acute kidney injury model with
a fluorescent/photoacoustic bimodal
molecular probe.
Front. Bioeng. Biotechnol. 10:1068533.
doi: 10.3389/fbioe.2022.1068533

COPYRIGHT
© 2022 Chen, Yuwen, Zhao, Li, Chen
and Liu. This is an open-access article
distributed under the terms of the
[Creative Commons Attribution License
\(CC BY\)](https://creativecommons.org/licenses/by/4.0/). The use, distribution or
reproduction in other forums is
permitted, provided the original
author(s) and the copyright owner(s) are
credited and that the original
publication in this journal is cited, in
accordance with accepted academic
practice. No use, distribution or
reproduction is permitted which does
not comply with these terms.

In situ detection of alkaline phosphatase in a cisplatin-induced acute kidney injury model with a fluorescent/photoacoustic bimodal molecular probe

Xingwang Chen¹, Zhiyang Yuwen¹, Yixing Zhao¹, Haixia Li^{1*},
Kang Chen^{1,2*} and Hongwen Liu^{1,2*}

¹Department of Hepatobiliary Surgery, The First Affiliated Hospital of Hunan Normal University (Hunan Provincial People's Hospital), Hunan Normal University, Changsha, China, ²Key Laboratory of Chemical Biology and Traditional Chinese Medicine Research, College of Chemistry and Chemical Engineering, Hunan Normal University, Changsha, China

Kidneys play an important part in drug metabolism and excretion. High local concentration of drugs or drug allergies often cause acute kidney injury (AKI). Identification of effective biomarkers of initial stage AKI and constructing activable molecular probes with excellent detection properties for early evaluation of AKI are necessary, yet remain significant challenges. Alkaline phosphatase (ALP), a key hydrolyzing protease, exists in the epithelial cells of the kidney and is discharged into the urine following kidney injury. However, no studies have revealed its level in drug-induced AKI. Existing ALP fluorescent molecular probes are not suitable for testing and imaging of ALP in the AKI model. Drug-induced AKI is accompanied by oxidative stress, and many studies have indicated that a large increase in reactive oxygen species (ROS) occur in the AKI model. Thus, the probe used for imaging of AKI must be chemically stable in the presence of ROS. However, most existing near-infrared fluorescent (NIRF) ALP probes are not stable in the presence of ROS in the AKI model. Hence, we built a chemically stable molecular sensor (CS-ALP) to map ALP level in cisplatin-induced AKI. This novel probe is not destroyed by ROS generated in the AKI model, thus allowing high-fidelity imaging. In the presence of ALP, the CS-ALP probe generates a new absorbance peak at 685 nm and a fluorescent emission peak at 716 nm that could be used to "turn on" photoacoustic (PA) and NIRF imaging of ALP in AKI. Levels of CS-ALP build up rapidly in the kidney, and CS-ALP has been successfully applied in NIRF/PA bimodal *in vivo* imaging. Through the NIRF/PA bimodal imaging results, we demonstrate that upregulated expression of ALP occurs in the early stages of AKI and continues with injury progression.

KEYWORDS

oxidative stress, acute kidney injury, alkaline phosphatase, fluorescent probe, photoacoustic (optoacoustic) imaging

Introduction

Drug-induced acute kidney injury (AKI) leads to serious morbidity and mortality (Blatt and Liebman, 2013). In the AKI process, drugs, such as cisplatin, first induce oxidative stress, which is followed by lysosomal damage and apoptosis. A recent survey indicated that AKI often continues unabated (Hsu et al., 2013). Unfortunately, the therapeutic schedule for AKI has not been highly effective due to lack of efficient biomarkers for early diagnosis and incomplete understanding of AKI pathogenesis (Charlton et al., 2014). Current clinical testing generally depends on the detection of urea nitrogen and serum creatinine in serum samples, which are often untimely, insensitive, and an indirect indicator of AKI (Charlton et al., 2014). In recent years, there has been extensive research focused on identification and verification of effective biomarkers for AKI. Previous studies have listed both potential and validated biomarkers of AKI, including small molecules, reactive oxygen species ($O_2^{\bullet-}$, $ONOO^-$, and ClO^-), proteins, and enzymes (Liu H.-W. et al., 2020; Liu L. et al., 2020; Cheng et al., 2020; Huang and Pu, 2021). Among them, several enzymatic biomarkers, including N-acetyl- β -glucosaminidase (NAG), alanine aminopeptidase (AAP), and alkaline phosphatase (ALP), exist in the epithelial cells of the kidney and are discharged into the urine following kidney damage (Charlton et al., 2014). Additionally, fluorescent sensors have been developed for testing NAG, gamma glutamyl transferase (GGT), and AAP in AKI, and the results have demonstrated the overexpression of these enzymes in the early stages of AKI (Lv et al., 2018; Huang et al., 2019; Huang et al., 2020; Tan et al., 2021). However, the expression level of ALP in AKI has not been adequately assessed. Therefore, there is a need for construction of an activable molecular probe for detection of ALP in AKI to improve early detection of AKI.

ALP catalyzes the hydrolytic reaction and transphosphorylation of substrates. It is widely expressed, at low levels, in human tissues, including bone, liver, and kidney. However, its activity is remarkably increased in several human diseases (Orimo, 2010). Despite abundant research on ALP fluorescent probes (Supplementary Table S1, ESI) (Li et al., 2012; Zhou et al., 2016; Li et al., 2017; Liu et al., 2017; Liu et al., 2018; Zhang P. et al., 2019; Zhang Q. et al., 2019; Gao et al., 2019; Wang et al., 2021b), its role in AKI remains unclear due to the lack of a kidney-specific molecular probe. Furthermore, existing ALP fluorescent molecular probes are not suitable for testing and imaging of ALP in the AKI model. As summarized in Supplementary Table S1, previously developed near-infrared fluorescent (NIRF) ALP probes were based on cyanine dye, which is not stable in the presence of ROS in the AKI model; many studies have indicated that there is a large increase in ROS

in AKI (Scheme 1A) (Jia et al., 2016; Cheng et al., 2019; Cheng et al., 2021; Li et al., 2021). In addition, the existing probes are hydrophobic and metabolized by the liver; therefore, no probe enrichment can occur in the kidney (Huang et al., 2017; Chen et al., 2021; Du et al., 2021; Yang et al., 2021). Development of a novel ALP fluorescent probe that is water soluble, chemically stable, and useful for *in situ* monitoring of ALP activity in the AKI model remains a significant challenge.

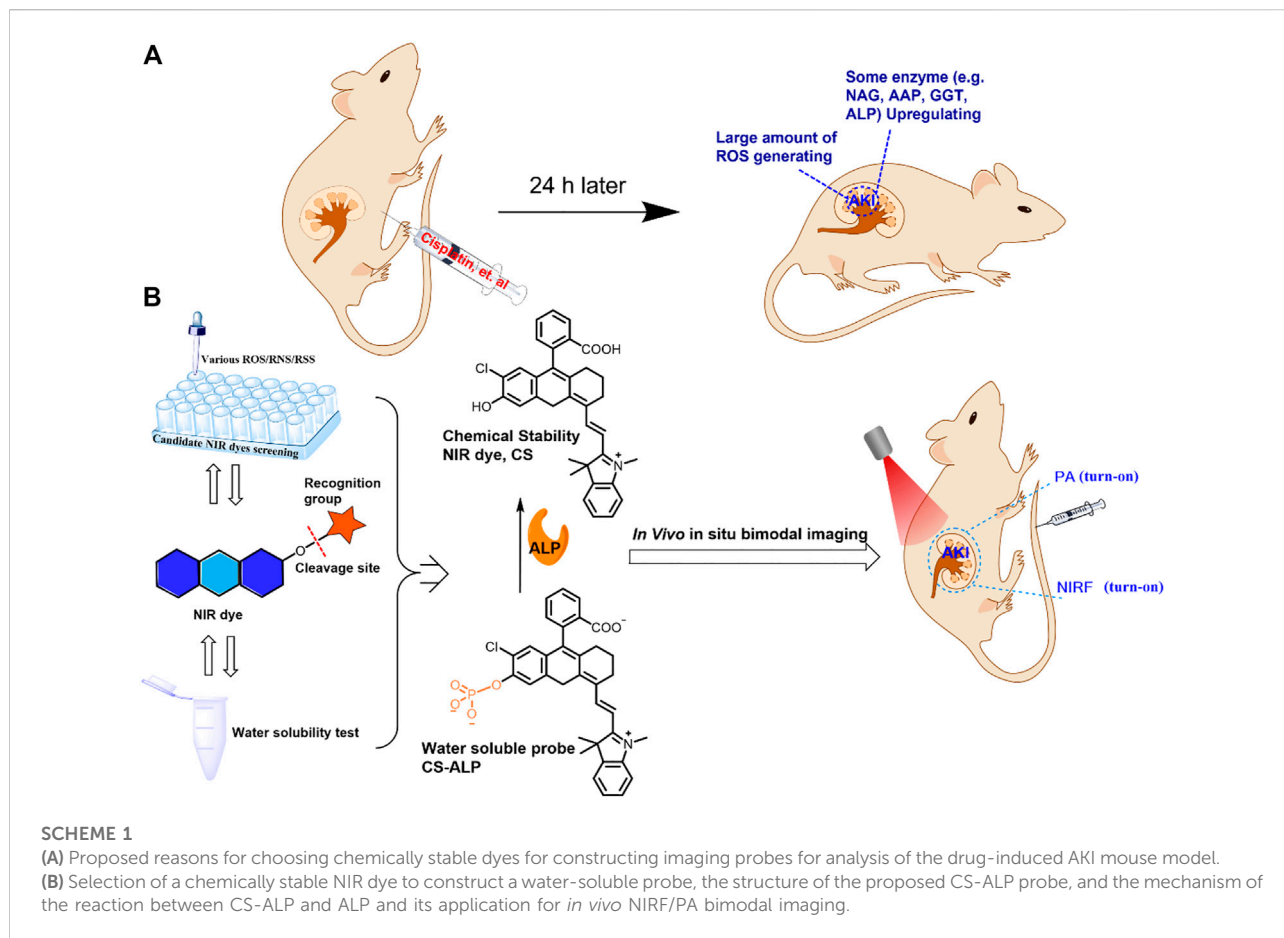
Herein, we report construction of a new NIRF probe, a chemically stable molecular sensor (CS-ALP), for studying AKI through measurement of ALP. CS-ALP was designed based on intramolecular charge transfer (ICT) and is composed of the chemically stable (CS) hemicyanine dye with a NIRF reporter and monophosphate linked to the hydroxyl group of the CS dye as an ALP cleavage site (Scheme 1B). Preliminary experiments and previous work have indicated that CS dye is stable in the presence of ROS at physiological concentration and shows mild water-solubility (Lv et al., 2018); thus, we chose CS dye for use in construction of an activable probe for high-fidelity imaging of ALP in AKI. In the presence of increasing concentrations of ALP, the monophosphate moiety is gradually hydrolyzed, resulting in gradual increase of the absorption maxima at 685 nm, which can be used for photoacoustic (PA) imaging. At the same time, the fluorescent emission peak at 716 nm was gradually enhanced, generating turn-on NIRF imaging. The probe displayed rapid response to ALP, high sensitivity (limit of detection: 0.26 U/L cal), and excellent specificity. Moreover, CS-ALP was successfully used for NIRF/PA bimodal imaging of ALP generated in cisplatin-stimulated human renal cortex proximal tubule epithelial cells (HK-2). Furthermore, using CS-ALP, the NIRF/PA bimodal *in vivo* visualization of ALP level in cisplatin-induced AKI was achieved for the first time, with results demonstrating that upregulated expression of ALP occurs at the early stages of AKI and continues with AKI progression.

Experimental design

General reagents and all required materials, instruments, the probe synthesis protocol, and experimental data are provided in the Supporting Information (ESI).

Spectrophotometric experiments

The probe was dissolved in DMSO to produce a stock solution (1.0×10^{-4} M). To obtain good optical performance of the probe, we used 5% DMSO as co-solvent. Since phosphate



could inhibit the activity of ALP, we used 10 mM tris-buffered saline (TBS, pH 8.0) for *in vitro* experiments. Both the UV-Vis absorption and fluorescent spectrum experiments were carried out in 10 mM TBS (pH 8.0). The fluorescent emission spectra were tested using a Hitachi F7000 spectrophotometer, with the excitation wavelength at 680 nm and the emission wavelength ranging from 700 to 900 nm. The test solutions were kept at 37°C for 30 min and then analyzed using spectrophotometry.

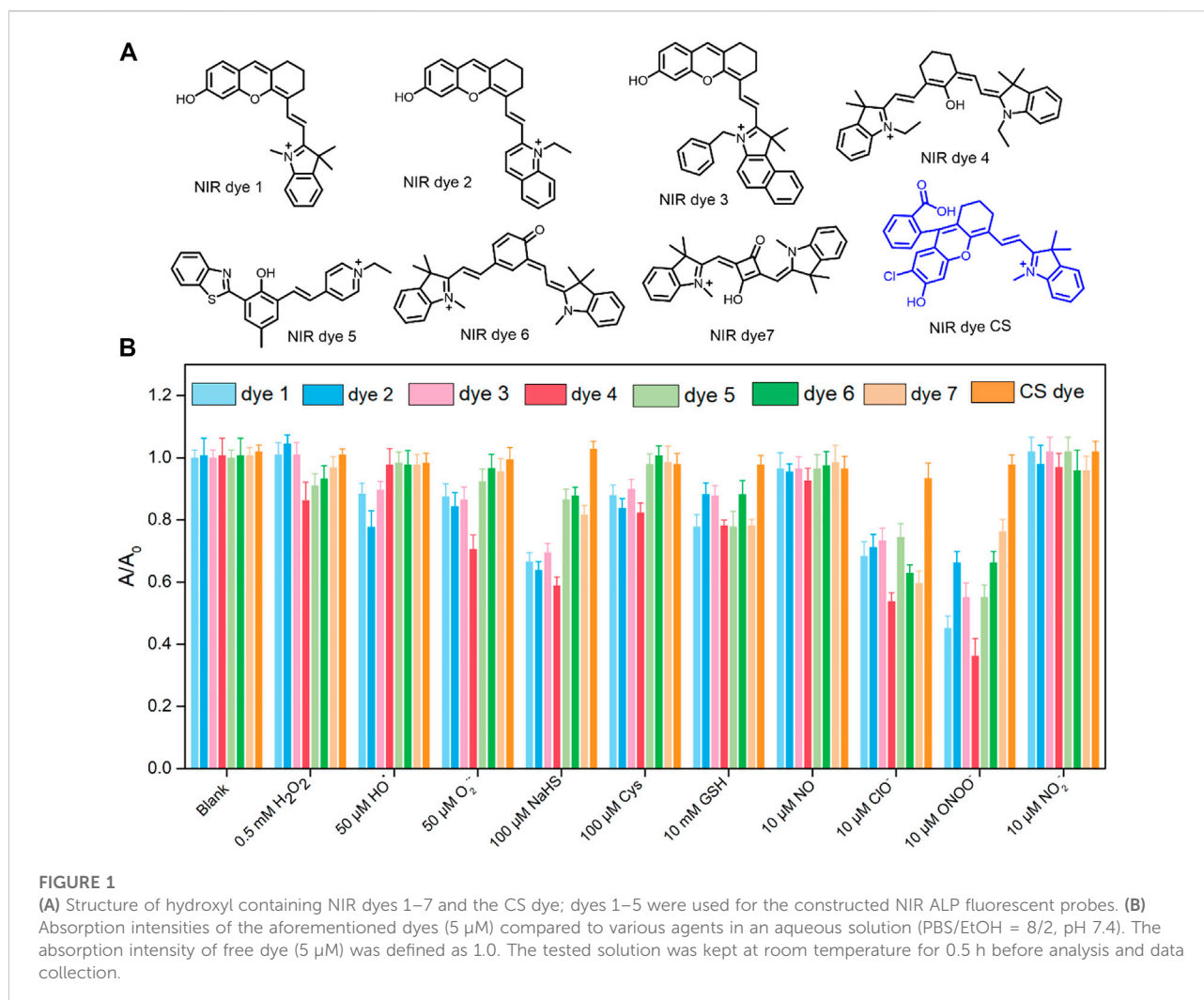
Fluorescence imaging in live cells

Cells were co-incubated with the probe in 10 mM TBS (pH 7.4). Cytotoxicity was assessed using the MTS assay. Cells were seeded in a 25-mm glass-bottom dish and grown for 24 h to approximately 85% confluency, followed by the live-cell confocal imaging experiments, for which the cells were divided into three groups as follows. The first group included HeLa cells that were incubated with 5 μM CS-ALP for 30 min. The cells were then washed with TBS buffer before imaging. In the second group, after pretreatment with Na₃VO₄ for 4 h, HeLa cells were incubated with 5 μM CS-ALP for 0.5 h and then washed with

TBS prior to imaging. The third group included control cells without CS-ALP. For the cisplatin-induced nephrotoxicity model in HK-2 cells, the experiment was divided into four groups. The first group included HK-2 cells that were treated with 5 μM CS-ALP. The second and third groups included HK-2 cells that were incubated with cisplatin, 500 μM or 1000 μM, for 4 h, respectively, and then co-incubated with 5 μM CS-ALP for 0.5 h. The fourth group included cells that were pre-incubated with 50 μM Na₃VO₄ in the presence of cisplatin (1 mM) for 4 h and then treated with 5 μM CS-ALP for 0.5 h. Confocal fluorescence imaging of cells was performed using an Olympus FV1000 laser confocal microscope (Japan).

Cisplatin-induced acute kidney injury

The drug-induced AKI mouse model was constructed following methods detailed in our previous report. Liu et al. (2020a) cisplatin was dissolved in 0.9% saline. BALB/c mice were intraperitoneally preinjected with cisplatin (20 mg/kg) for 24 h or 48 h. Live cells and live mouse experiments were in agreement with institutional animal care and use regulations, according to



protocol No. SYXK (Xiang) 2022-0007, approved by Laboratory Animal Center of Hunan.

Detection of ALP in urine and blood samples collected from the cisplatin-induced AKI mouse model

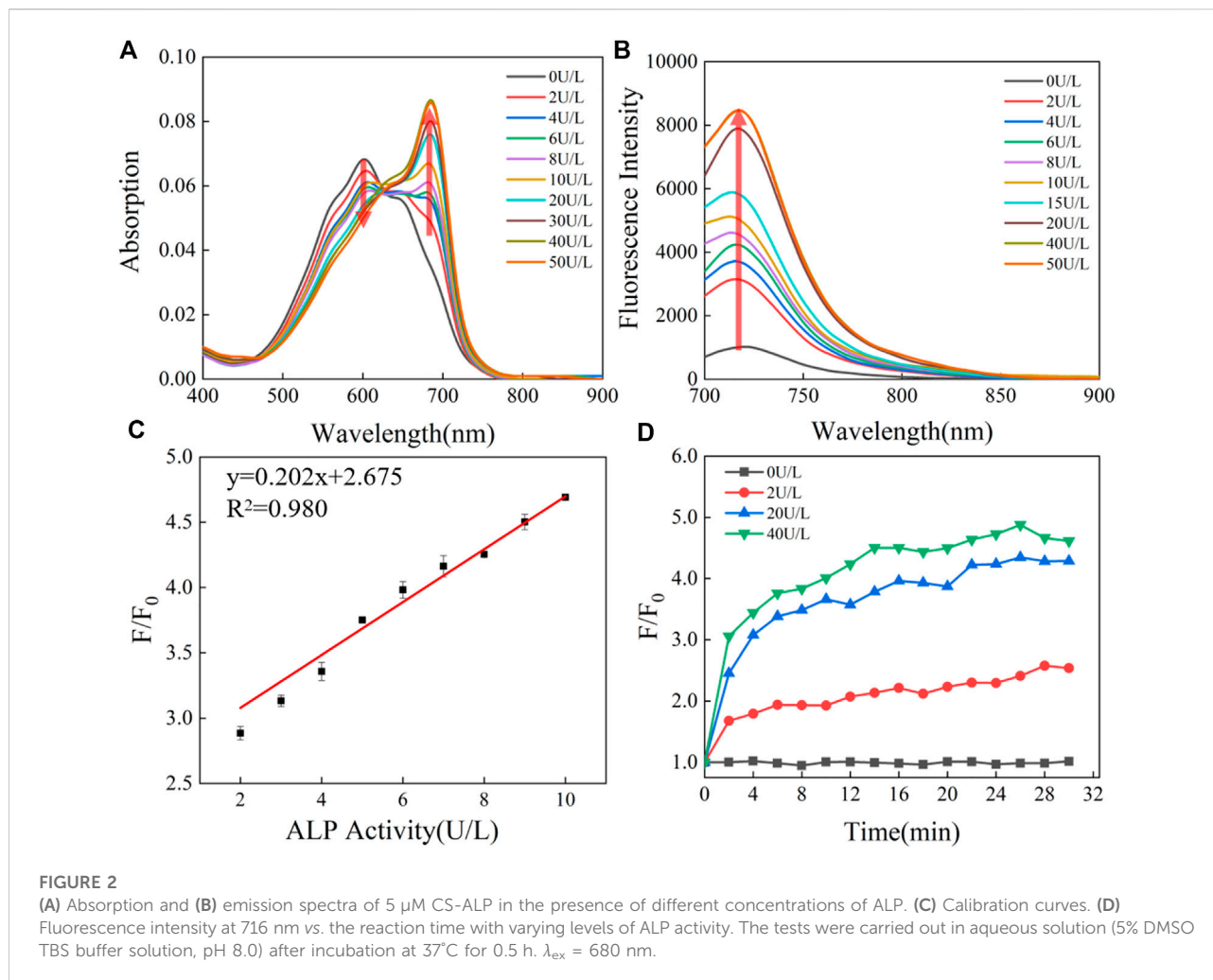
Six BALB/c mice, with average initial body weight of 20 g, were fed in a metabolic cage after intraperitoneal preinjection of cisplatin (20 mg/kg), with urine samples collected at 24 h and 48 h after injection. Blood samples were drawn *via* the retro-orbital sinus at 24 h and 48 h after intraperitoneal administration of cisplatin. The samples were then tested immediately by adding 50 or 100 μ L of the urine or blood sample to the test solution (total volume 1 ml) followed by recording of the fluorescence emission spectrum. The urine and blood of healthy mice were also tested as controls.

Determination of ALP in urine and blood samples using the commercially available ALP probe 4-methylumbelliferyl phosphate (4-MUP)

The 4-MUP probe was purchased from Sigma. The ALP level in urine and blood samples was then determined by measuring the fluorescence emission peak at 450 nm with λ_{ex} at 360 nm using a 4-MUP probe.

In vivo imaging of ALP in the cisplatin-induced AKI mouse

After intraperitoneal administration of cisplatin (20 mg/kg) for 24 h or 48 h, the CS-ALP probe (0.15 mg/kg in 20% DMSO/saline solution) was intravenously injected. The probe could not be completely solubilized in water at such a high concentration, so DMSO was added to improve solubility. Next, *in vivo* NIRF and PA imaging were carried out.

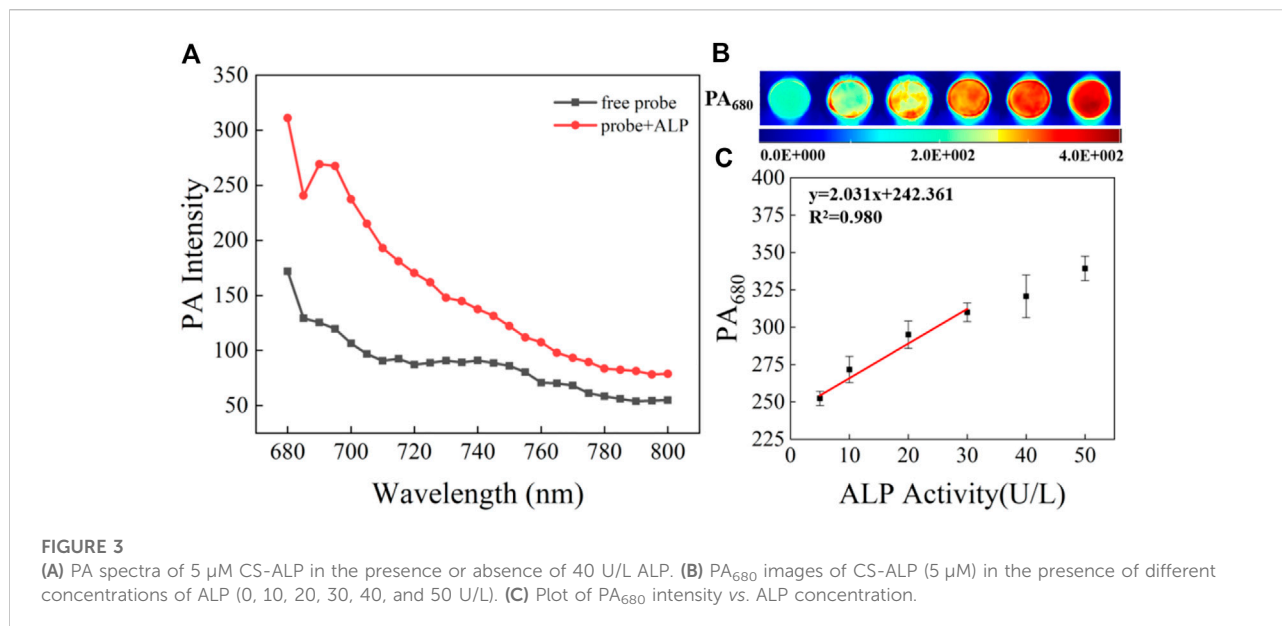


Results and discussion

Optimized design and synthesis of CS-ALP

Drug-induced AKI is accompanied by oxidative stress. Many studies have indicated that high levels of ROS are generated by cells under oxidative stress (Mao et al., 2017; Mao et al., 2022). Thus, the probe used for imaging of AKI must be chemically stable in the presence of ROS. As proof of concept, we first studied the reactivity of the CS dye with typical oxidants and nucleophiles, including H_2S , Cys, GSH, H_2O_2 , $\text{O}_2^{\bullet-}$, $\bullet\text{OH}$, ONOO^- , and ClO^- . As exhibited in Figure 1, the absorption intensity of CS at 685 nm remained unchanged with the addition of test species at physiological concentrations. In contrast, seven other kinds of NIR dyes, five of which (dyes 1–5) have been used for constructing NIR ALP fluorescent probes (Li et al., 2012; Li et al., 2017; Zhang P. et al., 2019; Zhang Q. et al., 2019; Gao et al., 2019; Wang et al., 2021b), were also tested. The results indicated that dyes 1–7 were not stable in the presence of $\text{O}_2^{\bullet-}$, $\bullet\text{OH}$,

ONOO^- , and ClO^- . These ROS have been shown to increase in concentration during drug-induced AKI (Lv et al., 2018; Huang et al., 2020). The results demonstrated that the existing NIRF ALP probes are not suitable for *in vivo* imaging and measurement of ALP levels in the drug-induced AKI model. In addition, for AKI *in vivo* imaging, probes must be water soluble at low concentration to allow enrichment in the kidney. We generated the probe through phosphorylation of the hydroxyl group of the CS fluorophore. The log P values of the probe and CS dye were 2.238 and 3.644, respectively, under pH 8.0 buffer conditions; as a control, the log P value of rhodamine B, a well known water-soluble dye, was calculated to be 2.032 under the experimental condition. The log P values indicated that CS-ALP has good water solubility and the potential for use in imaging to assess renal metabolism. To our knowledge, CS-ALP is the first molecular probe suitable for NIRF/PA bimodal *in vivo* detection of ALP in drug-induced AKI. The synthesis methodology for CS-ALP is shown in Supplementary Scheme S1, with structures assessed by ^1H NMR and MS (ESI).



Spectral response of the probe to ALP

After synthesizing the probe, we conducted a spectral study of the reaction between CS-ALP and ALP. CS-ALP showed a maximum absorption peak at 600 nm. After addition of ALP, a new absorption peak appeared at 685 nm. The increased absorption intensity displayed a good linear relationship with the activity of ALP at 0–10 U/L (Figure 2A, and Supplementary Figure S1, ESI). Concomitantly, the fluorescence emission peak at 716 nm grew dramatically upon increased ALP activity (Figure 2B). According to the fluorescence titration experiment, the fluorescence intensity at 716 nm exhibited a good linear relationship with ALP at 0–10 U/L (Figure 2C), with a calculated detection limit of 0.26 U/L. The catalytic activity of the probe in response to ALP was then assessed. Figure 2D depicts the fluorescence dynamics of the reaction of the probe to ALP at different concentrations (0, 2, 20, and 40 U/L). The results indicate that high-activity ALP allows the probe to crack quickly, resulting in a dramatic increase in fluorescence intensity. The fluorescence intensity of the reaction system is essentially balanced at about 26 min. At the same time, in the absence of ALP, there was no significant change in the fluorescence intensity of the reaction system (Supplementary Figure S2, ESI), and the photo-stability of the probe and the CS dye is good (Supplementary Figure S3). Together, these results indicate that CS-ALP is stable at physiological pH and could be applied in bioimaging.

To further demonstrate the specificity of the reaction between CS-ALP and the enzyme, the specificity of the probe for various potentially biologically relevant substances was

assessed. As shown in Supplementary Figure S4, the signal intensity is not significantly affected by other biological interference. Na_3VO_4 , a commonly used and competitive phosphatase inhibitor (Liu et al., 2017), was then co-incubated with ALP for 30 min before addition of the probe to the test solution. As shown in Supplementary Figure S5, addition of 50 μM Na_3VO_4 resulted in a significant reduction in fluorescence intensity. These results confirm that ALP-induced phosphate group-specific cleavage of the probe contributes to the enhancement of fluorescence intensity. Next, the effect of pH on CS-ALP and the enzymatic reaction was also evaluated, with results demonstrating that CS-ALP could perform well at physiological pH (Supplementary Figure S6).

The detectability of CS-ALP using PA imaging was then tested. We first tested the PA spectra for CS-ALP in the presence of varied ALP activity. The results showed that it was generally consistent with its absorption spectra. As displayed in Figure 3A, the PA signal intensity at 680 nm (PA_{680}) exhibited 1.8-fold enhancement at the saturation point. PA_{680} images of CS-ALP were obtained (Figure 3B) by treating the probe with increasing concentrations of ALP (0–30 U/L). The PA_{680} signals displayed linear responses to ALP in the 0–30 U/L concentration range, with a calculated detection limit of 2.5 U/L (Figure 3C).

Imaging of ALP in the cisplatin-induced AKI cell model

The cytotoxicity of CS-ALP was first assessed using the MTS assay. The results showed that high cell viability was maintained

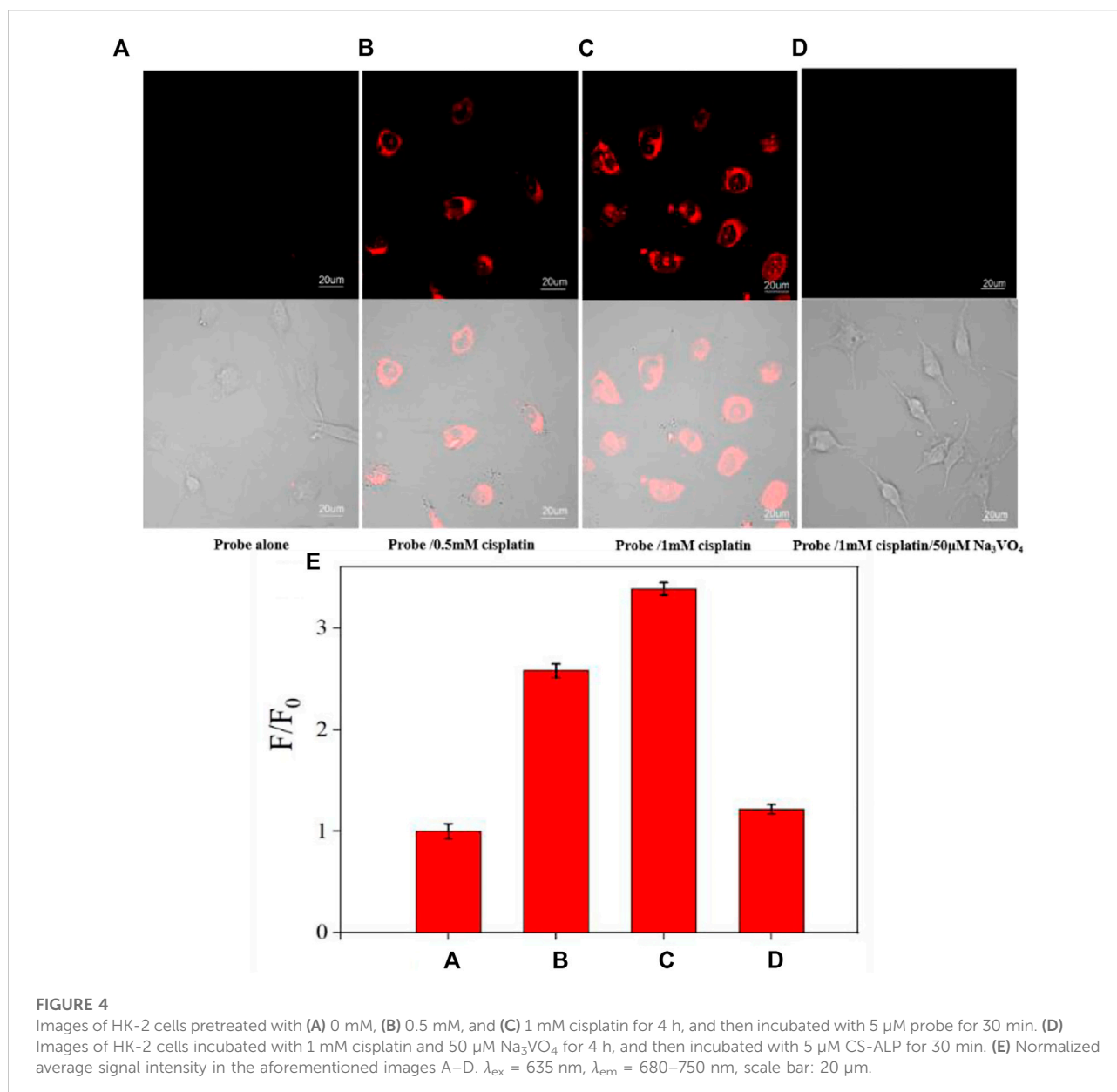


FIGURE 4

Images of HK-2 cells pretreated with (A) 0 mM, (B) 0.5 mM, and (C) 1 mM cisplatin for 4 h, and then incubated with 5 μM probe for 30 min. (D) Images of HK-2 cells incubated with 1 mM cisplatin and 50 μM Na₃VO₄ for 4 h, and then incubated with 5 μM CS-ALP for 30 min. (E) Normalized average signal intensity in the aforementioned images A–D. $\lambda_{\text{ex}} = 635 \text{ nm}$, $\lambda_{\text{em}} = 680\text{--}750 \text{ nm}$, scale bar: 20 μm.

after co-incubation with 2–10 μM probe, indicating that CS-ALP had good biocompatibility (Supplementary Figure S7). Next, we used HeLa cells for co-incubation with the probe for live-cell imaging experiments because ALP is overexpressed in HeLa cells. As shown in Supplementary Figure S8, when excited at 635 nm, HeLa cells showed bright fluorescence. However, when pretreated with Na₃VO₄ before co-incubation with CS-ALP, HeLa cells showed negligible fluorescence. The results demonstrate that the signal enhancement in HeLa cells is due to ALP activity. We then constructed an AKI cell model using cisplatin, a drug known to induce AKI. HK2 cells treated with CS-ALP alone were excited at 635 nm and

showed virtually no fluorescence (Figure 4A). At the same time, we observed that, when pretreating HK2 cells with 0.5 mM or 1 mM cisplatin, signal variations indicated cisplatin dose dependence (Figures 4B,C) and the fluorescence intensity ratio increased by 2.6 and 3.4 times, respectively (Figure 4E). Furthermore, when the cisplatin-treated HK2 cells were co-incubated with Na₃VO₄ for 30 min before addition of CS-ALP, there was almost no fluorescence (Figure 4D). These results suggest that CS-ALP could be used for measurement of endogenous ALP in cisplatin-treated HK2 cells, and that the activity of ALP is directly related to the process of cisplatin-induced AKI.

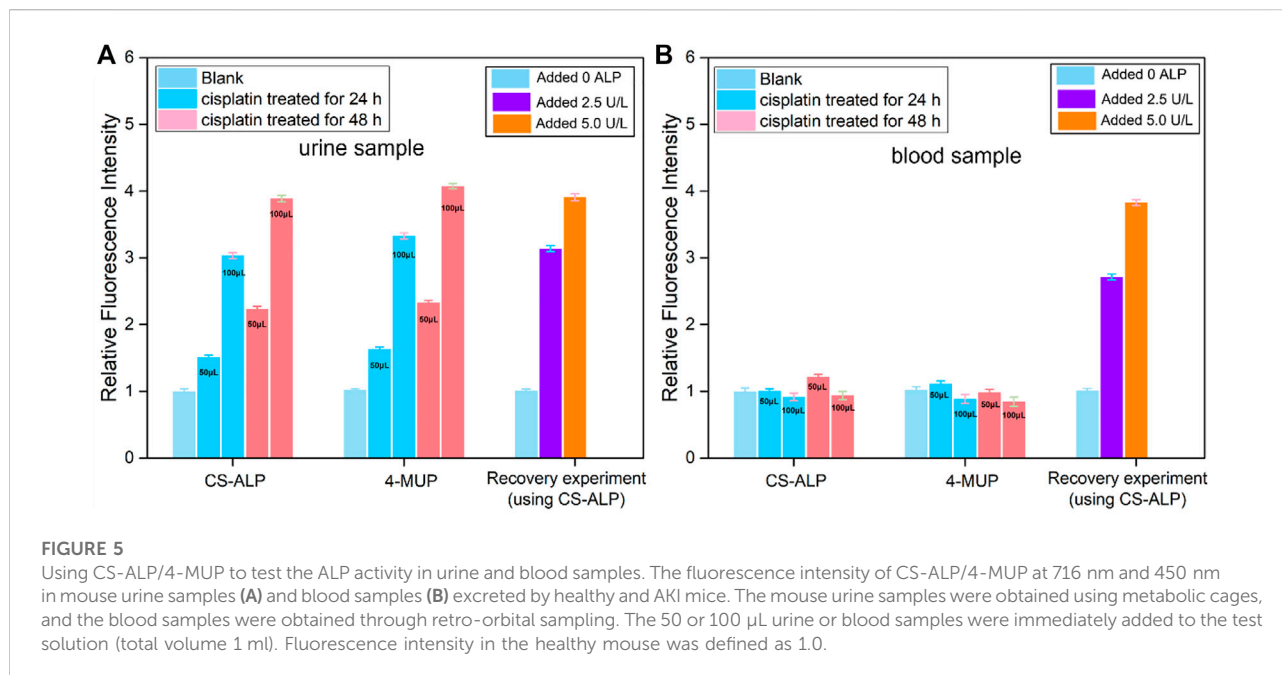


FIGURE 5

Using CS-ALP/4-MUP to test the ALP activity in urine and blood samples. The fluorescence intensity of CS-ALP/4-MUP at 716 nm and 450 nm in mouse urine samples (A) and blood samples (B) excreted by healthy and AKI mice. The mouse urine samples were obtained using metabolic cages, and the blood samples were obtained through retro-orbital sampling. The 50 or 100 μ L urine or blood samples were immediately added to the test solution (total volume 1 ml). Fluorescence intensity in the healthy mouse was defined as 1.0.

Detection of ALP in urine and blood samples collected from drug-induced AKI mouse

The AKI mouse model was established by intraperitoneal injection of 20 mg/kg cisplatin or normal saline as control. We first tested the urine samples of mice and found that the signal intensity from mice treated with cisplatin for 24 h and 48 h was 1.51-fold and 2.23-fold higher, respectively, than that of the control group. Blood sample analysis showed limited signal increase in the experimental groups compared to control. This result is consistent with that observed when using the commercially available ALP probe 4-MUP (Figure 5). These results are also consistent with a previous study showing that ALP was discharged into the urine following cellular injury due to early stage AKI (Charlton et al., 2014). According to the fluorescence correction curve for CS-ALP to ALP, the calculated ALP activity levels in the urine of AKI mice were 30.1 U/L (cisplatin-treated 24 h) and 45.6 U/L (cisplatin-treated 48 h), respectively. Thus, the CS-ALP probe may be an effective tool for early detection of AKI.

Bimodal NIRF/PA imaging of ALP in the drug-induced AKI mouse

After successful NIRF imaging of ALP in the AKI cell model, we applied CS-ALP to *in vivo* bimodal NIRF/PA imaging using commercial *in vivo* imaging systems. First, we

constructed an AKI mouse model according to our previous protocol (Liu H.-W. et al., 2020). The biodistribution of CS-ALP after intravenous (i.v.) injection showed that CS-ALP remained inactive in the control mouse but was activated in the AKI model mouse (Supplementary Figure S9A). In another group, imaging of isolated organs of the AKI mouse at 1.5 h post injection showed that CS-ALP accumulated primarily in the kidneys and liver (Supplementary Figure S9B), indicating that cisplatin may induce liver injury and kidney injury at the same time (Palipoch and Punsawad, 2013). As mentioned earlier, the log P value of CS-ALP is 2.238, which indicates that the probe has good water solubility and shows the potential for use in imaging to assess renal metabolism. Subsequently, 0.15 mg/kg CS-ALP was intravenously administered at different cisplatin post-treatment time points (24, 48, and 72 h). Real-time *in vivo* imaging showed that CS-ALP could be rapidly activated in the kidneys at 10 min post injection and that the signal intensity was stable at 10–30 min, followed by an obvious decrease at 120 min post injection (Supplementary Figure S10). Therefore, we timed the *in vivo* NIRF imaging to be at 30 min after injection of the probe. As displayed in Figures 6A,B, the NIRF signal intensity gradually enhanced, mainly in the kidneys of mice treated with cisplatin for 24 h or 48 h. The signal ratios for the 24 h and 48 h groups were 3.52-fold and 3.92-fold higher, respectively, than that of control group, indicating that ALP was upregulated in the kidneys of cisplatin-treated mice. We also carried out PA imaging, and the results are shown in Figure 6C and Supplementary Figure S11. The PA imaging data indicate that the kidney regions of the control group (treated with normal saline) were low contrast at

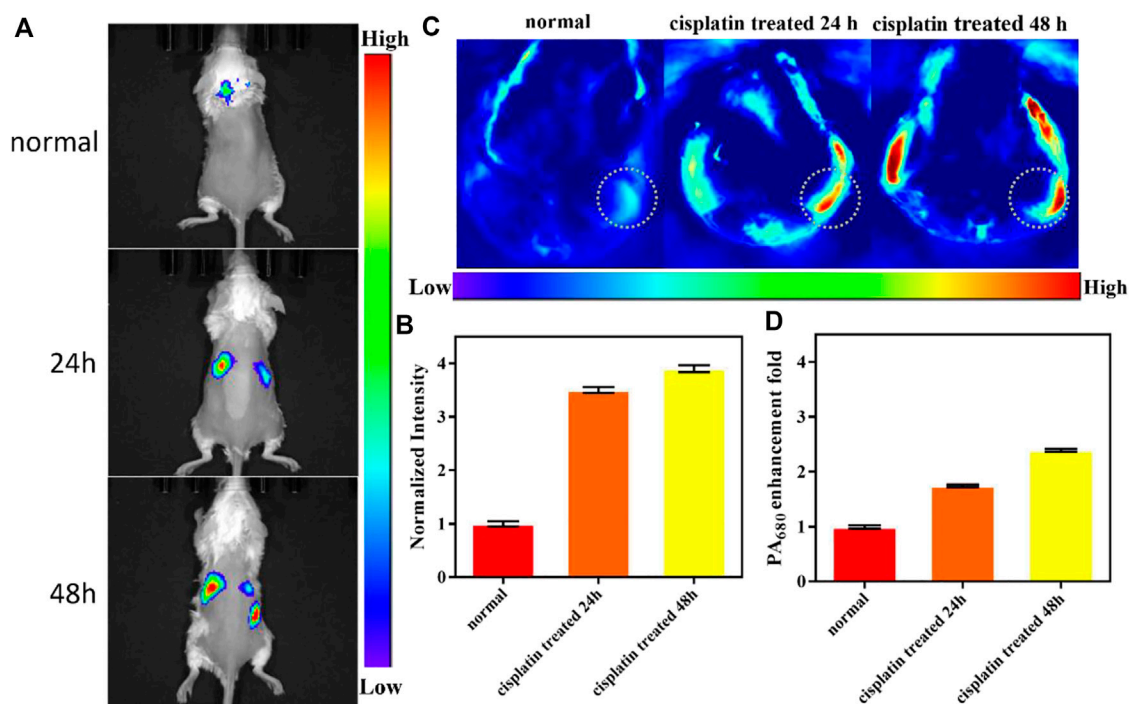


FIGURE 6

(A) *In vivo* imaging of a mouse after treatment with saline or cisplatin (20 mg/kg) for 24 h or 48 h, followed by injection (i.v.) of 0.15 mg/kg CS-ALP (in DMSO/DPBS, 1:4 v/v) for 20 min. Excitation filter 640, emission filter ICG. (B) Mean intensity ratio in (A). (C) PA_{680 nm} images from the kidneys of mice after pre-injection (i.p.) with saline or cisplatin (20 mg/kg) for 24 h or 48 h, followed by injection (i.v.) of 0.15 mg/kg CS-ALP (in DMSO/DPBS, 4:1 v/v) for 1 h. (D) Mean intensity ratio in (C). Values are the mean ± SD, $n = 3$.

1 h post injection of CS-ALP, while the PA signal in the kidney regions of cisplatin-treated mice gradually increased. The average signal intensity is displayed in Figure 6D, which indicates that the probe could be used for semi-quantitative analysis of ALP in drug-induced AKI. The PA imaging results were consistent with the NIRF imaging results, but the *in vivo* PA imaging required a longer time to obtain high contrast results compared to NIRF imaging due to the high background signal with PA imaging in this region, hence the advantage of dual-mode imaging for acquisition of more reliable *in vivo* imaging results (Luo et al., 2020; Zhang et al., 2020). Hematoxylin–eosin (H&E) staining revealed normal tubular morphology in the control group, compared to widely spaced tubules, damage to the brush border, and formation of hyaline casts within the damaged tubules in the experimental group 24 h after treatment with cisplatin (Supplementary Figure S12). Considering these results, we conclude that upregulation of ALP expression will occur at the early stages of AKI and will continue to be expressed with the progression of AKI. Additionally, we demonstrated the development and validation of use of CS-ALP in NIRF/PA bimodal imaging as a tool for evaluating drug-induced AKI in response to ALP.

Conclusion

In summary, we constructed a NIRF/PA bimodal sensor CS-ALP for the detection and imaging of ALP in cisplatin-induced AKI that has high sensitivity and specificity both *in vitro* and *in vivo*. The probe is chemically stable in the presence of ROS at physiological concentrations and allows high-fidelity imaging results. Upon addition and with increasing activity of ALP, the absorption intensity of the probe at 685 nm gradually increased and was accompanied by a NIRF enhancement with a peak at 716 nm, which were used for “turn-on” PA and NIRF imaging, respectively. According to the fluorescence titration experiment, the calculated detection limit was 0.26 U/L. CS-ALP was used in the imaging of ALP in HK2 cells after stimulation by cisplatin. Furthermore, CS-ALP is water-soluble and showed good renal-targeting capability for NIRF/PA bimodal imaging of ALP in a cisplatin-induced AKI mouse model. The results also indicate that upregulated expression of ALP occurs at early stages of AKI and continues with the progression of AKI. Our work in development of the CS-ALP bimodal molecular probe will not only facilitate mechanistic study of the roles of ALP in drug-induced AKI but may also assist in early diagnosis of AKI.

Data availability statement

The original contributions presented in the study are included in the article/Supplementary Material; further inquiries can be directed to the corresponding authors.

Ethics statement

The animal study was reviewed and approved by No. SYXK (Xiang) 2022-0007, approved by Laboratory Animal Center of Hunan.

Author contributions

XC: Investigation, methodology, data curation, and writing—original draft. ZY: Offered much help in the process of experiments. KC: Review and editing. HL: Funding acquisition. HL: Data curation, conceptualization, supervision, funding acquisition, and writing—review and editing.

Funding

This work was supported by the National Natural Science Foundation of China (Grant 22104036); the Project of Improving the Diagnosis and Treatment Capacity of Hepatobiliary, Pancreas and Intestine Diseases in Hunan Province (Xiangwei

References

- Blatt, A. E., and Liebman, S. E. (2013). Drug induced acute kidney injury. *Hosp. Med. Clin.* 2, e525–e541. doi:10.1016/j.ehmc.2013.04.003
- Charlton, J. R., Portilla, D., and Okusa, M. D. (2014). A basic science view of acute kidney injury biomarkers. *Nephrol. Dial. Transpl.* 29, 1301–1311. doi:10.1093/ndt/gft510
- Chen, Y., Pei, P., Lei, Z., Zhang, X., Yin, D., and Zhang, F. (2021). A promising NIR-II fluorescent sensor for peptide-mediated long-term monitoring of kidney dysfunction. *Angew. Chem. Int. Ed. Engl.* 60, 15943–15949. doi:10.1002/ange.202103071
- Cheng, D., Peng, J., Lv, Y., Su, D., Liu, D., Chen, M., et al. (2019). De novo design of chemical stability near-infrared molecular probes for high-fidelity hepatotoxicity evaluation *in vivo*. *J. Am. Chem. Soc.* 141, 6352–6361. doi:10.1021/jacs.9b01374
- Cheng, D., Xu, W., Gong, X., Yuan, L., and Zhang, X.-B. (2021). Design strategy of fluorescent probes for live drug-induced acute liver injury imaging. *Acc. Chem. Res.* 54, 403–415. doi:10.1021/acs.accounts.0c00646
- Cheng, P., Miao, Q., Huang, J., Li, J., and Pu, K. (2020). Multiplex optical urinalysis for early detection of drug-induced kidney injury. *Anal. Chem.* 92, 6166–6172. doi:10.1021/acs.analchem.0c00989
- Du, B., Chong, Y., Jiang, X., Yu, M., Lo, U.-G., Dang, A., et al. (2021). Hyperfluorescence imaging of kidney cancer enabled by renal secretion pathway dependent efflux transport. *Angew. Chem. Int. Ed. Engl.* 60, 355–363. doi:10.1002/ange.202010187
- Gao, X., Ma, G., Jiang, C., Zeng, L., Jiang, S., Huang, P., et al. (2019). *In vivo* near-infrared fluorescence and photoacoustic dual-modal imaging of endogenous alkaline phosphatase. *Anal. Chem.* 91, 7112–7117. doi:10.1021/acs.analchem.9b00109
- [2019] No. 118); the Natural Science Foundation of Hunan Province (2022JJ40216); the Natural Science Foundation of Changsha City (kq2202447); and the Postgraduate Scientific Research Innovation Project of Hunan Province (CX20190341).
- Hsu, R. K., McCulloch, C. E., Dudley, R. A., Lo, L. J., and Hsu, C.-y. (2013). Temporal changes in incidence of dialysis-requiring AKI. *J. Am. Soc. Nephrol.* 24, 37–42. doi:10.1681/asn.2012080800
- Huang, J., Huang, J., Cheng, P., Jiang, Y., and Pu, K. (2020). Near-infrared chemiluminescent reporters for *in vivo* imaging of reactive oxygen and nitrogen species in kidneys. *Adv. Funct. Mat.* 30, 2003628. doi:10.1002/adfm.202003628
- Huang, J., Lyu, Y., Li, J., Cheng, P., Jiang, Y., and Pu, K. (2019). A renal-clearable duplex optical reporter for real-time imaging of contrast-induced acute kidney injury. *Angew. Chem. Int. Ed. Engl.* 58, 17960–17968. doi:10.1002/ange.201910137
- Huang, J., and Pu, K. (2021). Near-infrared fluorescent molecular probes for imaging and diagnosis of nephro-urological diseases. *Chem. Sci.* 12, 3379–3392. doi:10.1039/d0sc02925d
- Huang, J., Weinfurter, S., Daniele, C., Perciaccante, R., Federica, R., Della Ciana, L., et al. (2017). Zwitterionic near infrared fluorescent agents for noninvasive real-time transcutaneous assessment of kidney function. *Chem. Sci.* 8, 2652–2660. doi:10.1039/c6sc05059j
- Jia, X., Chen, Q., Yang, Y., Tang, Y., Wang, R., Xu, Y., et al. (2016). FRET-Based mito-specific fluorescent probe for ratiometric detection and imaging of endogenous peroxynitrite: Dyad of Cy3 and Cy5. *J. Am. Chem. Soc.* 138, 10778–10781. doi:10.1021/jacs.6b06398
- Li, L., Ge, J., Wu, H., Xu, Q.-H., and Yao, S. Q. (2012). Organelle-specific detection of phosphatase activities with two-photon fluorogenic probes in cells and tissues. *J. Am. Chem. Soc.* 134, 12157–12167. doi:10.1021/ja3036256
- Li, S.-J., Li, C.-Y., Li, Y.-F., Fei, J., Wu, P., Yang, B., et al. (2017). Facile and sensitive near-infrared fluorescence probe for the detection of endogenous alkaline phosphatase activity *in vivo*. *Anal. Chem.* 89, 6854–6860. doi:10.1021/acs.analchem.7b01351

Conflict of interest

The authors declare that the research was conducted in the absence of any commercial or financial relationships that could be construed as a potential conflict of interest.

Publisher's note

All claims expressed in this article are solely those of the authors and do not necessarily represent those of their affiliated organizations, or those of the publisher, the editors, and the reviewers. Any product that may be evaluated in this article, or claim that may be made by its manufacturer, is not guaranteed or endorsed by the publisher.

Supplementary material

The Supplementary Material for this article can be found online at: <https://www.frontiersin.org/articles/10.3389/fbioe.2022.1068533/full#supplementary-material>

- Li, W., Shen, Y., Gong, X., Zhang, X.-B., and Yuan, L. (2021). Highly selective fluorescent probe design for visualizing hepatic hydrogen sulfide in the pathological progression of nonalcoholic fatty liver. *Anal. Chem.* 93, 16673–16682. doi:10.1021/acs.analchem.1c04246
- Liu, H.-W., Chen, L., Xu, C., Li, Z., Zhang, H., Zhang, X.-B., et al. (2018). Recent progresses in small-molecule enzymatic fluorescent probes for cancer imaging. *Chem. Soc. Rev.* 47, 7140–7180. doi:10.1039/c7cs00862g
- Liu, H.-W., Li, K., Hu, X.-X., Zhu, L., Rong, Q., Liu, Y., et al. (2017). *In situ* localization of enzyme activity in live cells by a molecular probe releasing a precipitating fluorochrome. *Angew. Chem. Int. Ed. Engl.* 56, 11950–11954. doi:10.1002/ange.201705747
- Liu, H.-W., Zhang, H., Lou, X., Teng, L., Yuan, J., Yuan, L., et al. (2020a). Imaging of peroxynitrite in drug-induced acute kidney injury with a near-infrared fluorescence and photoacoustic dual-modal molecular probe. *Chem. Commun.* 56, 8103–8106. doi:10.1039/d0cc01621g
- Liu, L., Jiang, L., Yuan, W., Liu, Z., Liu, D., Wei, P., et al. (2020b). Dual-modality detection of early-stage drug-induced acute kidney injury by an activatable probe. *ACS Sens.* 5, 2457–2466. doi:10.1021/acssensors.0c00640
- Luo, X., Chen, M., and Yang, Q. (2020). Research progress on near infrared II technology for *in vivo* imaging. *Acta Chim. Sin.* 78, 373. doi:10.6023/a20020045
- Lv, Y., Dan, C., Dongdong, S., Chen, M., Yin, B.-C., Yuan, L., et al. (2018). Visualization of oxidative injury in the mouse kidney using selective superoxide anion fluorescent probes. *Chem. Sci.* 9, 7606–7613. doi:10.1039/c8sc03308k
- Mao, Z., Jiang, H., Li, Z., Zhong, C., Zhang, W., and Liu, Z. (2017). An N-nitrosation reactivity-based two-photon fluorescent probe for the specific *in situ* detection of nitric oxide. *Chem. Sci.* 8, 4533–4538. doi:10.1039/c7sc00416h
- Mao, Z., Xiong, J., Wang, P., An, J., Zhang, F., Liu, Z., et al. (2022). Activity-based fluorescence probes for pathophysiological peroxynitrite fluxes. *Coord. Chem. Rev.* 454, 214356. doi:10.1016/j.ccr.2021.214356
- Orimo, H. (2010). The mechanism of mineralization and the role of alkaline phosphatase in health and disease. *J. Nippon. Med. Sch.* 77, 4–12. doi:10.1272/jnms.77.4
- Palipoch, S., and Punsawad, C. (2013). Biochemical and histological study of rat liver and kidney injury induced by cisplatin. *J. Toxicol. Pathol.* 26, 293–299. doi:10.1293/tox.26.293
- Tan, J., Yin, K., Ouyang, Z., Wang, R., Pan, H., Wang, Z., et al. (2021). Real-time monitoring renal impairment due to drug-induced AKI and diabetes-caused CKD using an NAG-activatable NIR-II nanoprobe. *Anal. Chem.* 93, 16158–16165. doi:10.1021/acs.analchem.1c03926
- Wang, W.-X., Jiang, W.-L., Guo, H., Li, Y., and Li, C.-Y. (2021b). Real-time imaging of alkaline phosphatase activity of diabetes in mice *via* a near-infrared fluorescent probe. *Chem. Commun.* 57, 480–483. doi:10.1039/d0cc07292c
- Yang, C., Wang, H., Yokomizo, S., Hickey, M., Chang, H., Kang, H., et al. (2021). ZW800-PEG: A renal clearable zwitterionic near-infrared fluorophore for potential clinical translation. *Angew. Chem. Int. Ed. Engl.* 60, 13966–13971. doi:10.1002/ange.202102640
- Zhang, P., Fu, C., Zhang, Q., Li, S., and Ding, C. (2019a). Ratiometric fluorescent strategy for localizing alkaline phosphatase activity in mitochondria based on the ES IPT process. *Anal. Chem.* 91, 12377–12383. doi:10.1021/acs.analchem.9b02917
- Zhang, Q., Li, S., Fu, C., Xiao, Y., Zhang, P., and Ding, C. (2019b). Near-infrared mito-specific fluorescent probe for ratiometric detection and imaging of alkaline phosphatase activity with high sensitivity. *J. Mat. Chem. B* 7, 443–450. doi:10.1039/c8tb02799d
- Zhang, Y., Wang, Y., Yang, X., Yang, Q., Li, J., and Tan, W. (2020). Polyaniline nanovesicles for photoacoustic imaging-guided photothermal-chemo synergistic therapy in the second near-infrared window. *Small* 16, 2001177. doi:10.1002/sml.202001177
- Zhou, J., Du, X., Yamagata, N., and Xu, B. (2016). Enzyme-instructed self-assembly of small d-peptides as a multiple-step process for selectively killing cancer cells. *J. Am. Chem. Soc.* 138, 3813–3823. doi:10.1021/jacs.5b13541